# Galileo IOV RTK positioning: standalone and combined with GPS

Dennis Odijk[1], Peter J.G. Teunissen[1,2], Amir Khodabandeh[1]

[1]GNSS Research Centre

Curtin University

GPO Box U1987

Perth, WA 6845, Australia

[2]Department of Geoscience and Remote Sensing

Delft University of Technology

PO Box 5048

2628 CN Delft, The Netherlands

Email: d.odijk@curtin.edu.au

# Abstract

Results are presented of real-time kinematic (RTK) positioning based on carrier-phase and code (pseudorange) observations of the four Galileo In-Orbit Validation (IOV) satellites, as they were in orbit and transmitting navigation data at the time of writing this article (2013). These Galileo data were collected by multi-GNSS receivers operated by Curtin University and as such this article is one of the first presenting results of short-baseline ambiguity resolution and positioning based on Galileo IOV observations. The results demonstrate that integer ambiguity resolution based on the four IOV satellites needs fewer than three minutes when at least observables from three frequencies are used. Combined with data of four GPS satellites even instantaneous (single epoch) ambiguity resolution is demonstrated, using only two frequencies per constellation (i.e. E1+E5a & L1+L2). We also show that at locations with obstructed satellite visibility, such that positioning based on either GPS-only or Galileo-only becomes impossible or only in a very inaccurate way, combined Galileo&GPS positioning is feasible, within 10 minutes if one frequency of each constellation is used and only 2 minutes time-to-fix the ambiguities based on observations of two frequencies of each constellation. It is furthermore demonstrated that this results in positions with centimeter-level accuracy in the horizontal plane and sub-decimeter accuracy in the vertical direction.



**Keywords:** Galileo IOV, GPS, GNSS, interoperability, RTK positioning, ambiguity resolution, LAMBDA method

# 1. Introduction

Europe's global navigation satellite system (GNSS) Galileo is currently under development. At the moment of writing this article (2013) the project is in its In-Orbit Validation (IOV) phase. As part of this phase four IOV satellites have been launched (the first pair on 21 October 2011 and the second pair one year later, on 12 October 2012) and are in orbit. These first four IOV satellites have to demonstrate that the space and ground infrastructure of Galileo meet the requirements and they have to validate the system's design in advance of completing the full constellation **[1]**. The full Galileo constellation will consist of 30 satellites in three orbital planes, including three in-orbit spare ones. The first two satellites, IOV-PFM (PRN E11) and IOV-FM2 (PRN E12), began transmitting navigation messages in January 2013. The second pair of IOV satellites, IOV-FM3 (PRN E19) and IOV-FM4 (PRN E20) started to transmit their navigation messages in March 2013. Table 1 gives the frequencies/wavelengths of the Open Service signals that can be tracked from the Galileo IOV satellites, vs. those of the signals that can be tracked from the satellites of the established Global Positioning System (GPS). It is assumed that data on the following Galileo frequencies are tracked: E1, E5a, E5b and E5. The E6 signal was not tracked by the receivers used in our analyses. We remark that this signal will not be part of Galileo's Open Service, as it will be encrypted for commercial purposes **[2].**

The Galileo E5 signal, with its Alternative Binary Offset Carrier (AltBOC) modulation, is an extra-wideband signal having two components, E5a and E5b, and these can be received by tracking them as two independent BPSK(10) modulations, at center frequencies 1176.45 MHz and 1207.14 MHz. Secondly, the E5a and E5b bands can be tracked coherently as one signal,

centered at the mean of the E5a and E5b frequencies, leading to high-performance E5 observables **[3]**. The wideband E5 signal is expected to have a much better code (pseudorange) accuracy and multipath suppression as compared to its subcarriers E5a and E5b **[4]**. From Table 1, note that two of Galileo's frequency bands overlap GPS; as such, the Galileo E1 and E5a frequencies are identical to the L1 and L5 frequencies of GPS.

Since the first transmission of the Galileo IOV signals in December 2011, several research and industry groups have started to analyse and work with the signals **[5]**. First positioning results based on Galileo IOV data combined with GPS were presented in **[6]**; however the results were based on the first IOV satellite only. Precise point positioning based on the first two IOV satellites in combination with the two GIOVE satellites was demonstrated in **[7]**, where they used satellite orbit and clock information from the Cooperative Network for GNSS Observation (CONGO; **[8]**). In a follow-up article **[9]** first results are given for single point positioning as well as relative phase-based kinematic positioning based on the four Galileo IOV satellites. Again, orbits and clocks were determined from the CONGO network, and stations that are part of the Multi-GNSS Experiment (MGEX) of the International GNSS Service (IGS) **[10]**.

This article focusses on high-precision real-time kinematic (RTK) positioning results based on data of the four IOV satellites for which their positions are computed using the broadcast navigation message data. Crucial to RTK positioning is a correct fixing of the carrier-phase ambiguities, and, according to the authors' knowledge, results of Galileo IOV ambiguity resolution, standalone as well as with GPS, are described in an article for the very first time. The Galileo IOV data have been collected by the permanent multi-GNSS receivers operated

by Curtin University in Perth, Western Australia. The focus of the article will be on the time needed to reliably fix the carrier-phase ambiguities for different combinations of the Galileo frequencies. Integer ambiguity resolution is the prerequisite for precise positioning and hence should be as fast as possible. Results of ambiguity resolution and positioning were not only evaluated for Galileo IOV alone, but also when combined with GPS. This was done for two periods of about 2 hours in which the four IOV satellites were simultaneously observed in Perth. These two datasets are separated by 10 days, corresponding to the period after which the four-satellite Galileo constellation is repeating itself **[11]**. In addition, combined Galileo&GPS positioning results will be presented for another dataset mimicking urban canyon conditions, such that it would not be possible to obtain precise positioning results based on data of one constellation only.

This article is set up as follows. The observation models underlying Galileo-only or GPS-only and combined Galileo&GPS as based on double differences are reviewed in Section 2. Section 3 presents results of ambiguity resolution and positioning based on these models, while Section 4 ends the article with conclusions.

## 2. Single GNSS vs. combined GPS&Galileo positioning model

*Single GNSS double-differenced observation model*

The double-differenced (DD) observation equations for a single GNSS constellation short-baseline positioning model are given as follows, in linearized form, for a certain epoch *i* **[12, 13]**:

$$
\begin{aligned}
E\{\phi_j^{1_* s}(i)\} &= -[\mathbf{u}^{1_* s}(i)]^T \mathbf{b}(i) \quad + \lambda_j a_j^{1_* s} \\
E\{p_j^{1_* s}(i)\} &= -[\mathbf{u}^{1_* s}(i)]^T \mathbf{b}(i)
\end{aligned}
\qquad (1)
$$

where $E\{\cdot\}$ denotes the mathematical expectation operator and where $(\cdot)_j^{1_* s} = (\cdot)_j^s - (\cdot)_j^{1_*}$ is used to denote a DD observable or variable between a pair of receivers (note: $(\cdot)_j^s$ denotes a between-receiver single-differenced observable) and a pair of satellites, denoted as $s = 2_*, \ldots, m_*$ ($m_*$ denotes the number of satellites tracked), relative to a pivot satellite, denoted as $1_*$. The asterisk (*) is introduced to distinguish between the constellations, i.e. * = *G* for GPS and * = *E* for Galileo. The frequency of the observables/variables is denoted using the index $j = 1_*, \ldots, f_*$, with $f_*$ the number of frequencies. DD phase and code (observed-minus-computed) observables for each frequency are denoted as $\phi_j^{1_* s}(i)$ and $p_j^{1_* s}(i)$, both in distance units. Unknown parameters are first the 3D baseline vector for each epoch (so the receivers may be in motion), denoted as $b(i)$ (in distance units). The line-of-sight unit vectors between receiver and satellites are denoted as $u^s(i)$ In Eq. (1) they appear in between-satellite form and are denoted as $u^{1_* s}(i) = u^s(i) - u^{1_*}(i)$.The second group of unknown parameters are the DD ambiguities for each frequency, denoted as $a_j^{1_* s}$, with the ambiguities in cycles. The DD ambiguities are integer and constant as long as no cycle slips occur. Their wavelengths are denoted as $\lambda_j$.

With a 'short' baseline we assume that the distance between the two GNSS receivers is at most about 10 kilometres long, see e.g. **[14]**. This has the following consequences. First, the

line-of-sight vectors can be taken identical for both receivers with respect to the same satellite. Second, errors in the satellite positions (that are assumed to be known in the baseline processing) can be safely ignored. Third, for short baselines the between-receiver differential atmospheric errors are so small that they can be ignored as well (under normal ionospheric conditions and in mid-latitude regions).

If we assume that the system of equations in Eq. (1) is set up for $i = 1,\ldots,k$ observation epochs and $j = 1_*,\ldots,f_*$ frequencies, the redundancy (number of observations minus number of parameters) of the single-constellation DD model equals $f_*(m_* - 1)(2k - 1) - 3k$. This implies that if we have phase and code observations of at least one epoch ($k \geq 1$) and at least one frequency ($f_* \geq 1$), the number of satellites is required to be at least four ($m_* \geq 4$). We remark in this context that although the precision of the code data is much lower than of the phase data, they strengthen the observation model. Without code data, it is not possible to solve the model based on a single epoch of data, as there would be more unknowns than observations using phase observations only.

*Combined GPS&Galileo observation model*

When GPS and Galileo observations are tracked by both receivers, the phase/code observation equations as in Eq. (1) can be set up for both systems, where they share the baseline components as common parameters. In such a combined observation model each of the systems defines its own pivot satellite to perform the differencing. This observation model will be referred to as the 'standard' GPS+Galileo model. However, GPS and Galileo have two identical frequencies (L1-E1 and L5-E5a) and we can take benefit of this. It is then possible to

difference the Galileo observations at each identical frequency with respect to a pivot satellite of *GPS* **[15]**. In that case between-receiver differenced *GPS-Galileo inter-system biases* (ISB) may remain after performing the double differencing. In **[16, 17]** it is mentioned that these differential ISBs are due to a difference in receiver hardware biases between the GPS and Galileo signals. In **[18]** it was demonstrated that for baselines consisting of receiver pairs of the same manufacturer and type the differential ISBs are absent, while for pairs of mixed receivers they are present but very stable in time, such that they can be calibrated. Although these results were based on data using the GIOVE satellites, it is expected that a similar conclusion holds for the IOV satellites.

An alternative combined (linearized) system of DD GPS and Galileo observation equations, in which the Galileo phase and code data at identical frequencies are differenced relative to the GPS pivot satellite and corrected for differential ISBs, can now be given as follows:

$$
\begin{array}{lcll}
E\{\phi_o^{1_G s}(i)\} & = & -[\mathbf{u}^{1_G s}(i)]^T \mathbf{b}(i) \quad +\lambda_o a_o^{1_G s} & ; \text{ GPS identical freq.} \\
E\{\phi_j^{1_G s}(i)\} & = & -[\mathbf{u}^{1_G s}(i)]^T \mathbf{b}(i) \quad +\lambda_j a_j^{1_G s} & ; \text{ GPS other freq.} \\
E\{\phi_o^{1_G 1_E}(i) - \lambda_o \hat{\delta}_o^{GE}\} & = & -[\mathbf{u}^{1_G 1_E}(i)]^T \mathbf{b}(i) \quad +\lambda_o a_o^{1_G 1_E} & ; \text{ GPS-Galileo identical freq. (pivot sats.)} \\
E\{\phi_o^{1_G q}(i) - \lambda_o \hat{\delta}_o^{GE}\} & = & -[\mathbf{u}^{1_G q}(i)]^T \mathbf{b}(i) \quad +\lambda_o a_o^{1_G q} & ; \text{ Galileo identical freq.} \\
E\{\phi_l^{1_E q}(i)\} & = & -[\mathbf{u}^{1_E q}(i)]^T \mathbf{b}(i) \quad +\lambda_l a_l^{1_E q} & ; \text{ Galileo other freq.} \\
E\{p_o^{1_G s}(i)\} & = & -[\mathbf{u}^{1_G s}(i)]^T \mathbf{b}(i) & ; \text{ GPS identical freq.} \\
E\{p_j^{1_G s}(i)\} & = & -[\mathbf{u}^{1_G s}(i)]^T \mathbf{b}(i) & ; \text{ GPS other freq.} \\
E\{p_o^{1_G 1_E}(i) - \hat{d}_o^{GE}\} & = & -[\mathbf{u}^{1_G 1_E}(i)]^T \mathbf{b}(i) & ; \text{ GPS-Galileo identical freq. (pivot sats.)} \\
E\{p_o^{1_G q}(i) - \hat{d}_o^{GE}\} & = & -[\mathbf{u}^{1_G q}(i)]^T \mathbf{b}(i) & ; \text{ Galileo identical freq.} \\
E\{p_l^{1_E q}(i)\} & = & -[\mathbf{u}^{1_E q}(i)]^T \mathbf{b}(i) & ; \text{ Galileo other freq.}
\end{array}
\tag{2}
$$

with the GPS satellite index $s = 2_G, \ldots, m_G$ and the Galileo satellite index $q = 2_E, \ldots, m_E$. Furthermore, the frequency indices are defined as follows: $o = 1, \ldots, f$ for the identical

frequencies between GPS and Galileo; $j = 1_G, \ldots, f_G$ for the other GPS frequencies and $l = 1_E, \ldots, f_E$ for the other Galileo frequencies. Thus, the notation $f_S$ (with $S \in \{G, E\}$) is used here to denote the frequencies per constellation that are not identical, while for a single constellation it was used to denote the *total* number of frequencies per GNSS. For example, assume we have two GPS frequencies and three Galileo frequencies in the combined model of which one frequency is identical, we have $f = 1$, $f_G = 1$ and $f_E = 2$. In case of the single constellation models we would have $f_G = 2$ and $f_E = 3$. The differential ISBs are defined as $\delta_o^{GE} = \delta_o^E - \delta_o^G$ for phase and as $d_o^{GE} = d_o^E - d_o^G$ for code, where $\delta_o^*$ and $d_o^*$ denote the between-receiver differenced hardware phase and code delay per constellation. Thus, $\delta_o^{GE}$ and $d_o^{GE}$ can be regarded as double differences with respect to the receivers and the different constellations. The corrections for these differential ISBs are denoted using the 'hat' sign in Eq. (2). While the DD ambiguities of the non-identical Galileo frequencies are relative to the Galileo pivot satellite, correction for the ISBs has as consequence that the DD ambiguities for the Galileo frequencies identical to those of GPS become relative to the pivot satellite of GPS.

The redundancy of the 'standard' combined model can be shown to read $[(f + f_G)(m_G - 1) + (f + f_E)(m_E - 1)](2k - 1) - 3k$. Now, with at least one epoch ($k \geq 1$), as well as at least one frequency per system ($f + f_G \geq 1$ and $f + f_E \geq 1$), we have the requirement for the *combined* number of satellites that $m_G + m_E \geq 5$. This condition can be met with several combinations of GPS and Galileo satellites, as long there is at least one satellite of each system. In the alternative combined model (2) there is one phase and code observation more (per overlapping frequency and per epoch; thus $2fk$) than in the standard

model. On the other hand, the number of additional unknowns in model (2) is of size $f$ (the number of DD ambiguities between the pivot satellites of both systems). For the redundancy this means that it is increased with $f(2k-1)$ compared to the redundancy of the 'standard' GPS+Galileo model. This implies that if $f \geq 1$ we can do with one satellite less compared to the standard model, i.e. $m_G + m_E \geq 4$. This more relaxed requirement may be an advantage in areas with low satellite visibility (e.g. urban canyons).

*Three-step procedure for solving the relative GNSS model*

To solve the relative receiver positions of the models in the previous subsections with high precision it is common to make use of the integer nature of the DD ambiguities. The model is then solved by means of a three-step procedure. In the first step the integer nature of the ambiguities is discarded and one performs a standard least-squares adjustment. The solution is referred to as the 'float' solution, and is –for short timespans– governed by the precision of the code data (the phase data only start to contribute after the receiver-satellite geometry has changed sufficiently). In the second step the part of the float solution corresponding to the ambiguities is input for the LAMBDA method **[19]**, which outputs an integer solution. It needs to be tested whether this integer solution can be accepted as the correct one with sufficient reliability. For this the Fixed-Failure rate Ratio Test (FFRT; **[20]**) is used, which also needs the second-best solution that is provided by the LAMBDA method, in addition to the 'best' or integer least-squares solution. After the integer ambiguities can be successfully resolved, in the third and final step another standard least-squares solution is carried out, with the ambiguities held fixed. The resulting position solution, often referred to as the 'fixed' solution, is then governed by the high precision of the phase data.

# 3. Results of ambiguity resolution and precise positioning

*Selection of Galileo IOV and GPS data: datasets I and II*

Galileo IOV and GPS data were collected by three multi-GNSS receivers permanently set up at Curtin University in Perth, Australia. Two Trimble TRM59800.00 geodetic antennas, with a short spacing of about 8.4 m, are connected to the roof of building 402; see Figure 1. One of the antennas is connected to a Trimble NetR9 receiver (CUTA), while the other antenna is connected to *two* receivers using a splitter: another Trimble NetR9 receiver (CUT0) and a Septentrio PolaRx4 receiver (CUT1). Both Trimble and Septentrio receivers collect Galileo data on four frequencies, and GPS data on three frequencies.

We first present ambiguity resolution and positioning results for a period of about 2 hours during which the four Galileo IOV satellites were tracked above an elevation of 10 degrees, i.e. for 20 March 2013 (04:05:30-06:00:00 GPST; where GPST stands for GPS Time), and compare these results for a period 10 days after, i.e. 30 March 2013 (03:24:00-05:18:30 GPST), when the Galileo constellation was the same to that of 20 March. These datasets are referred to as ‘dataset I’. Figure 2 (left) depicts the sky plot for the 2-hour periods during both days. In addition to the four Galileo satellites, the sky plot shows the tracks of four GPS satellites, which are used for the GPS-only computations and those combined with Galileo. Data of other than these four GPS satellites was collected as well, though not used in our computations; otherwise GPS would have a too dominant contribution to the combined solution. To have a ’fair’ comparison we selected those four GPS satellites that were observed continuously during the 2-hour timespan.

To get insight in the receiver-satellite geometry, Figure 3 (left) shows the position dilution of precision (PDOP) values based on these four GPS satellites, as well as those based on the four Galileo IOV satellites, plus the PDOPs corresponding to combined Galileo&GPS. The PDOPs of GPS-only are very close to those of Galileo-only: while those of GPS have a mean of about 4, the Galileo-only PDOPs are just below this value. The combined Galileo&GPS case is most favorable in terms of receiver-satellite geometry, with PDOPs varying between a low 2 and 3. Besides PDOP values, Figure 4 shows the DOPs for the east component (EDOP), the north component (NDOP) and the up or vertical component (VDOP). While the VDOP is in all cases (i.e. Galileo-only, GPS-only and Galileo&GPS) larger than the EDOP or NDOP during the 2-hour timespan, note that for the Galileo-only case the NDOP is always larger than the EDOP.

In addition to the results based on a cut-off elevation of 10 degrees, results are presented based on Galileo and GPS observations at a much higher cut-off elevation, i.e., 45 degrees, to mimic ‘urban canyon’ conditions with obstructed satellite visibility at low elevations. These data are referred to as ‘dataset II’. Figure 2 (right) shows the sky plot corresponding to a period of 1.3 hours (17:54:00-19:13:00 GPST) on the day of 8 April 2013, during which two Galileo IOV satellites and three to four GPS satellites were available above this high elevation. Most of the time only three GPS satellites were tracked simultaneously; the required number of four GPS satellites needed for positioning was only available for 53% of the time. The accuracy of positioning based on these four GPS satellites would be very poor, because the receiver-satellite geometry turns out to be very bad, as indicated by the extremely large PDOP values in Figure 3 (right). Although in the Galileo&GPS case at least 5 satellites

are available all the time, which is sufficient for positioning, the PDOP of combined positioning still reaches up to values of 30, mainly close to epoch 50. Table 2 summarizes the timespans and satellites that are used in datasets I and II.

*Measuring the performance of ambiguity resolution and positioning*

Although both receivers of the baselines are stationary, in the processing the baseline coordinates are treated to be unlinked in time. The availability of these relative positions with high accuracy depends on the speed at which the ambiguities can be resolved to their correct integer values. Instantaneous (single-epoch) ambiguity resolution is fastest, but can only be successful if the underlying model is strong enough. Otherwise, more epochs of data need to be processed in order for the float ambiguity solution to converge and integer estimation can be successful. The ambiguities are resolved successfully if the fixed-failure rate ratio test is passed. In all computations a fixed failure rate of 0.001 was used. The time needed for correct integer ambiguity estimation will be referred to as 'time-to-fix-ambiguities' (TTFA). To assess the performance of the positioning, the estimated ambiguity-float and ambiguity-fixed positions are compared to their given highly accurate benchmark positions. These benchmark positions are obtained from processing long time series of GPS data for the stations.

*Stochastic model of the Galileo IOV and GPS data*

The stochastic model of the Galileo and GPS code data, as has been adopted in all computations in this article, is determined using variance-component estimation **[21]** based on the observation data of 20 and 30 March 2013, but then extended with one hour during which the four IOV satellites were visible as well, as to have more data to reliably estimate the variance components. Next to the variance components, also the (cross) covariances between

the observables are estimated, which is in particular relevant for the Galileo E5a, E5b, and E5 observables, which are all derived from the same wideband signal.

Because of the known a-priori coordinates of the short baselines, together with the cancelling of the differential atmospheric delays, the observables in DD mode can be treated as zero-mean random signals. Taking the exponential elevation weighting strategy **[22]**, the weighted average of the squared elements of each observable type would then be referred to as an estimate of the observable type's variance. Similarly, the estimates of the cross-covariance between the observable types are computed through weighted averaging the product of their elements which, in turn, yields their estimated correlation coefficients.

Table 3 presents the estimated code standard deviations, referenced to zenith and in undifferenced mode, of the Galileo and GPS observables for both Trimble and Septentrio receivers. We remark that the GPS L5 frequency is not used in the computations since at the moment of writing this article (2013) it is transmitted by just three operational GPS satellites. Table 4 presents the results of the estimated (zenith-referenced) *correlation coefficients* of the Galileo code observables of the Trimble receivers. It can be seen that the results between the two days are very consistent with each other. Furthermore, the estimated correlation coefficients in Table 4 are reasonably small; the largest values of about 0.3 are the correlation coefficients between E5a and E5, as well as between E5b and E5. Based on these results, we believe that it is permitted to assume that the Galileo observables of different frequencies are uncorrelated. From the results it also followed that the code data of GPS can be assumed uncorrelated. For the correlation coefficients of the code data tracked by the Septentrio receiver a similar conclusion could be drawn as for the Trimble receivers. Concerning the

phase data, based on the estimated variances it turned out that the undifferenced phase standard deviation for all observables could be set to a value of 3 mm (in zenith).

The estimated zenith-referenced standard deviations for phase and code are multiplied by an exponential function, cf. **[22]**, as to model the precision as a function of elevation. In a next step the propagation law of variances is applied to compute the variance-covariance matrix of the DD observations.

## 3.1 Results dataset I: four satellites per constellation

For the two days forming dataset I the times to fix the integer ambiguities are evaluated for several cases: Galileo-only, GPS-only and Galileo&GPS combined. To quantify the benefit of additional frequencies, in the computations we started with single-frequency cases and systematically added one frequency at a time. Figure 5 presents the mean convergence times to fix the ambiguities for the two baselines, i.e. CUT0-CUTA, consisting of identical Trimble receivers, and CUT1-CUTA, the mixed Septentrio-Trimble baseline. For the CUT0-CUTA baseline two times-to-fix are shown in Figure 5: the first corresponding to 20 March and the second to 30 March. Unfortunately, the Septentrio receiver did not track data on the first day (20 March), so for the baseline CUT1-CUTA only the times-to-fix corresponding to 30 March are shown. For the CUT0-CUTA baseline it can be seen that the differences in times-to-fix between the two days are very small. Generally, the ambiguity convergence times for baseline CUT1-CUTA are slightly better than those of baseline CUT0-CUTA, which is attributed to

the better code precision for some of the observables tracked by the Septentrio receiver(see Table 3).

*Single-constellation single-frequency ambiguity resolution performance*

As can be seen from Figure 5, for both baselines the single-constellation (i.e. Galileo-only or GPS-only) single-frequency cases require the longest times-to-fix, which is due to the weakness of the underlying model, since satellite or frequency redundancy is absent. For the Galileo E1 observations even the two-hour timespan is insufficient to resolve the ambiguities. From GPS-only we know that single-frequency ambiguity resolution is only expected to be successful with a large number of satellites **[23]**, and thus only four visible satellites is simply too few. Comparing the Galileo-only E1 case with E5a, E5b and E5, it can be seen that E1 performs much worse (even the full two hour timespan is still not enough for ambiguity resolution), as compared to the E5a, E5b and E5 frequencies. This result is due to the shorter wavelength of E1 (~19 cm) as compared to the other three (~25 cm), which led to a poorer float ambiguity solution for E1. The much better performance of E5 (about 19 minutes time-to-fix) is attributed to the low code noise of this signal; a promising feature which was also emphasized in **[3]**, although in that article simulated Galileo observations were used. The time-to-fix-ambiguities in case of GPS-only L1 are for the two baselines approximately one hour, and this is much shorter than for the Galileo-only E1 case. At first sight, this better result for GPS-only may look surprising; since the precision of the E1 and L1 observations is comparable and the geometry based on the four GPS satellites is slightly poorer than based on the four Galileo satellites, as demonstrated by the higher PDOP values for GPS-only in Figure 3. However, one has to keep in mind that it is not so much the *instantaneous* geometry that is relevant for ambiguity resolution, but more importantly is its *change in time* **[24]**. While the

instantaneous geometry is poorer for GPS than for Galileo, the PDOP of GPS changes more than that of Galileo, which remains at a more constant level during the two-hour timespan. This change of the geometry has a favorable effect on the precision of the float GPS ambiguities, leading to shorter times-to-fix as compared to the Galileo-only case, for which there is less change in receiver-satellite geometry.

*Single-constellation dual-frequency ambiguity resolution performance*

Adding a second frequency already improves the single-constellation ambiguity times-to-fix considerably, to less than ten minutes for Galileo-only (E1+E5a and E1+E5, with a better performance for the second combination), and to even less than two minutes for GPS-only. The explanation for the better results in case of GPS-only is the same as in the single-frequency case.

*Galileo-only triple and quadruple-frequency ambiguity resolution performance*

Before discussing the performance of combined Galileo&GPS ambiguity resolution and positioning, we will give results for Galileo-only ambiguity resolution when a third and fourth frequency are added. From Figure 5 it follows that the addition of a third frequency still improves the ambiguity convergence time somewhat. For both baselines the time-to-fix is 2-3 minutes when based on either the E1+E5a+E5b observables, or the E1+E5a+E5 observables. The inclusion of the precise E5 observables does not have much influence in the triple-frequency performance compared to the use of E5b, as the times-to-fix are already at a fast level. Adding a fourth frequency (i.e. E1+E5a+E5b+E5) gives the best performance for Galileo-only: the mean time-to-fix-ambiguities is less than two minutes.

*Galileo&GPS single/multi-frequency ambiguity resolution performance*

In the combined Galileo&GPS case, single-frequency (E1&[1]L1) ambiguity resolution was first based on the 'standard' model with a pivot satellite for each constellation (see Section 2). For both baselines the resulting mean time-to-fix is less than three minutes. Compared to the single-system performances, which are on the order of one to a few hours, this is a tremendous improvement. An even further improvement is possible when instead of two pivot satellites only one is used; for the baseline CUT0-CUTA, consisting of identical Trimble receivers, differential ISBs can be assumed absent; however, for the baseline CUT1-CUTA, consisting of mixed receivers, we first determined the differential ISBs from another dataset. The differential phase ISB was estimated at -0.21 cycle, while the differential code ISB was estimated at an insignificant value close to zero, implying that it can be neglected for this combination of Septentrio and Trimble receivers. Thus only the phase data received an a-priori ISB correction. From Figure 5 it can be seen that the resulting performance of ambiguity resolution based on one pivot satellite is very similar for both baselines: the mean time-to-fix for the ambiguities is about 1.5 minutes, about half the time of the two-pivot-satellite case. In a next step, for the combined Galileo&GPS multi-frequency case we processed two frequencies from both systems, i.e. E1+E5a and L1+L2. As can be expected, because of the strength of this model, its performance is best: for both baselines ambiguity resolution can be done successfully in an instantaneous way, thus based on a single epoch of data all the time.

*Positioning performance*

[1] The '&' symbol is used to list the observables of the combined Galileo&GPS constellations, whereas the '+' symbol is reserved to list the observables belonging to one constellation.

The above cases will now be used to assess the performance of the positioning. Figure 6 depicts the errors in east-north-up for the position solutions of CUTA, obtained from the Galileo E1+E5a, GPS L1+L2 and Galileo&GPS E1+E5a&L1+L2 processing of the CUT1-CUTA baseline, based on float as well as fixed ambiguities. These positioning results are plotted in multi-epoch mode, where for the float solution use is made of the time constancy of the ambiguities. The fixed position errors are only plotted after the correct integer ambiguities have been estimated (in the Galileo-only case this takes more time than in the GPS-only and Galileo&GPS cases; this explains why the fixed curve starts 'later' in the Galileo-only case). The position errors are obtained by subtracting the position estimates from the precisely known benchmark coordinates. For each component the empirical mean and root-mean-square (RMS) error values are shown in Table 5. It can first be seen that in the Galileo-only case the east component is determined with a better precision than the north component: its RMS error values are 5 cm for float and 3 mm for fixed east; while the RMS error is a large 27 cm for float north and about 6 mm for fixed north. This better precision is east direction is due to the actual receiver-satellite geometry: in Figure 4 (left) it can be seen that the EDOP in case of Galileo-only is smaller than the NDOP, indicating that the Galileo satellite distribution in east-west direction is much better than in north-south (as there are no satellites in the south). After ambiguity resolution however there is much less difference in the precision of east vs. north: both are at sub-cm level. In the GPS-only L1+L2 case, there is less difference in precision level of east and north components. Although the float solution shows a large bias during the timespan (the coordinate estimates show a mean of about 30 cm in all three components), the results look much better after ambiguity resolution, with the means of the fixed components at the sub-cm level. The bottom three graphs of Figure 6 depict the position errors for the combined Galileo&GPS case. Although ambiguity resolution can be done

instantaneously in this case, the positioning results are plotted in multi-epoch mode to compare them to the single-constellation positioning results. From Table 5 it can be seen that the combined case results in the lowest RMS error values for float and fixed: the float RMS error is smaller than 12 cm and the fixed RMS error is below 1 cm, for all three components.

## 3.2 Results dataset II: 'urban canyon' conditions

For dataset II, where Galileo&GPS observations that are tracked above 45 degrees elevation are used, we only present results of *combined* ambiguity resolution and positioning, because only two Galileo satellites were tracked and only four GPS satellites were available for half of the time (for the rest of the time just three GPS satellites), having a very poor geometry, see Figure 3 (right).

Figure 7 presents the mean time-to-fix the ambiguities during the timespan, for the same short baselines as used in dataset I, i.e. CUT0-CUTA, formed by two Trimble receivers, and CUT1-CUTA, formed by a Septentrio and a Trimble receiver.

For the single-frequency case, combining Galileo E1 with GPS L1, the processing was performed in two different ways: firstly, based on a pivot satellite per constellation (the 'standard' approach) and secondly, ignoring the differential ISBs for the CUT0-CUTA baseline, while applying differential ISB corrections to the CUT1-CUTA baseline, such that one pivot satellite (in this case of GPS) for both Galileo and GPS is sufficient. With two pivot satellites, the mean time-to-fix is in the range of 11-14 minutes, but this decreases to 7-10

minutes when one pivot satellite is used. These times are longer than for the similar cases in dataset I (see Figure 5), but this is due to the fewer satellites we have in dataset II, resulting in a weaker model. Adding a frequency for both constellations (i.e. E1+E5a and L1+L2) significantly shortens the ambiguity convergence time, to just above one minute for both baselines. Using the more precise E5, i.e. processing E1+E5 with L1+L2, improves ambiguity resolution, although the gain is only limited compared to the use of E5a: the mean time-to-fix is just below one minute for both baselines. While in case of dataset I *instantaneous* ambiguity resolution was feasible based on E1+E5a and L1+L2 observables, this is not possible for the current dataset as a result of the lack of satellite redundancy for many epochs. However, times-to-fix of less than one minute are promising for applications with obstructed satellite visibility. The addition of a third or even a fourth Galileo frequency does not further reduce the ambiguity convergence time, as compared to the case when two Galileo frequencies are used.

To illustrate the performance of the positioning based on a large cut-off elevation of 45 degrees, Figure 8 shows the east-north-up position errors for CUTA (relative to its precisely known coordinates), based on the Galileo&GPS single-frequency processing applying one pivot satellite (of GPS) for both constellations (for baseline CUT1-CUTA). It can be seen that the north component is determined with a higher accuracy in terms of RMS errors, followed by east and up. This is due to the receiver-satellite geometry for this dataset, with a better distribution of satellites in north-south direction than in east-west (see the sky plot at the right in Figure 2, showing that most satellites basically move in the north-south direction). Finally, we remark from Figure 8 that the formal standard deviation of the up component reaches up to 8 cm after ambiguity fixing. This relatively poor height precision is due to the large cut-off

elevation of 45 degrees, resulting in a receiver-satellite geometry in which all satellites are relatively close to the zenith.

# 4. Conclusions

This article has presented results of carrier-phase ambiguity resolution and high-precision relative positioning based on real observation data of the first four Galileo IOV satellites in orbit that were received beginning in March 2013. The positions of these Galileo satellites were computed using the ephemerides transmitted in the navigation messages. The performance of LAMBDA-based ambiguity resolution and positioning was tested for some short baselines for which the differential atmospheric delays and ephemeris errors can be safely ignored.

Although instantaneous (single-epoch) ambiguity resolution based on just four satellites is not possible, as the underlying model is too weak, it was demonstrated that dual-frequency Galileo-only ambiguity resolution needs less than ten minutes on average for the considered datasets. This mean time-to-fix was even reduced to less than two minutes using all four frequencies of Galileo's Open Service. Combined with dual-frequency data of four GPS satellites successful instantaneous Galileo&GPS ambiguity resolution could be demonstrated using at least dual-frequency Galileo data. The resulting (kinematic) positioning accuracy, based on fixed ambiguities, was at the few millimeter level horizontally and at the 1 centimeter level vertically, in terms of RMS errors. It is emphasized that these results are based on only four satellites of each constellation; in (future) practice the results will be even

better when there are more Galileo satellites. From our analyses it could furthermore be demonstrated that the precision of the E5 code observables is much better than of the code observables at the other frequencies of Galileo's Open Service (i.e. E1, E5a and E5b).

The benefits of the combination of Galileo with GPS will become even more evident in areas with poor visibility at low elevations ("urban canyon"), such that insufficient (i.e. fewer than four) GPS satellites are available, or they have a poor receiver-satellite geometry. Mimicking such conditions by setting the elevation cut-off to 45 degrees in our analyses, resulted in a mean ambiguity convergence time of only slightly more than one minute based on the combination of two frequencies of each constellation.

## Acknowledgments

This research was carried out in the context of the Australian Space Research Program (ASRP) project "Platform Technologies for Space, Atmosphere and Climate", as well as in the context of the Positioning Program Project 1.01 "New carrier phase processing strategies for achieving precise and reliable multi-satellite, multi-frequency GNSS/RNSS positioning in Australia" of the Cooperative Research Centre for Spatial Information (CRC-SI). The second author is the recipient of an Australian Research Council (ARC) Federation Fellowship (project number FF0883188). All this support is gratefully acknowledged.

## References

[1] European Space Agency (ESA, 2013). http://www.esa.int (consulted March 2013).

[2] European Union (2010). *European GNSS (Galileo) Open Service – Signal in Space Interface Control Document*. September 2010.

[3] Simksy, A., J.M. Sleewaegen, M. Hollreiser, and M. Crisci (2006). Performance assessment of Galileo ranging signals transmitted by GSTB-V2 satellites. *Proc. ION GNSS 2006*, Fort Worth, TX, 26-29 September, pp. 1547-1559.

[4] Diessongo, T.H., T. Schüler, and S. Junker (2013). Precise position determination using a Galileo E5 single-frequency receiver. *GPS Solutions,* DOI 10.1007/s10291-013-0311-2.

[5] Galileo in its glory. *GPS World,* Vol. 23, No. 1, January 2012, pp. 12-14.

[6] Kassabian, N., G. Falco, and L. Lo Presti (2012). First joint GPS/IOV-PFM Galileo PVT estimation using carrier phase measurements. *Proc. European Navigation Conference (ENC) 2012*, Gdansk, Poland, 25-27 April.

[7] Langley, R.B., S. Banville, and P. Steigenberger (2012). First results: precise positioning with Galileo prototype satellites. *GPS World,* Vol. 23, No. 9, September 2012, pp. 45-49.

[8] Montenbruck, O., A. Hauschild, and U. Hessels (2010). Characterization of GPS/GIOVE sensor stations in the CONGO network. *GPS Solutions,* Vol. 15, No. 3, pp. 193-205, DOI 10.1007/s10291-010-0182-8.

[9] Steigenberger, P., U. Hugentobler, and O. Montenbruck (2013). First demonstration of Galileo-only positioning. *GPS World,* Vol. 24, No. 2, February 2013, pp. 14-15.

[10] International GNSS Service Multi-GNSS Experiment (2013). http://igs.org/mgex (consulted April 2013).

[11] Zandbergen, R., S. Dinwiddy, J. Hahn, E. Breeuwer, and D. Blonski (2004). Galileo orbit selection. *Proc. ION GNSS 2004*, Long Beach, CA, 21-24 September, pp. 616-623.

[12] Teunissen, P.J.G., and A. Kleusberg (eds.) (1998). *GPS for Geodesy*, 2nd edition, Springer-Verlag, Berlin Heidelberg New York.

[13] Hofmann-Wellenhof, B., H. Lichtenegger, and E. Wasle (2008). *GNSS – Global Navigation Satellite Systems, GPS, GLONASS, Galileo and more*, Springer-Verlag, Wien New York.

[14] Chang, X.W., C.C. Paige, and L. Yin (2004). Code and carrier phase based short baseline GPS positioning. *GPS Solutions,* Vol. 7, No. 4, pp. 230-240. DOI 10.1007/s10291-003-0077-z.

[15] Julien, O., P. Alves, M.E. Cannon, and W. Zhang (2003). A tightly coupled GPS/Galileo combination for improved ambiguity resolution. *Proc. European Navigation Conference (ENC) 2003*, Graz, Austria, 22-25 April. Available at *http://plan.geomatics.ucalgary.ca/papers/gnss2003_atightlycoupledgpsgalileo.pdf*.

[16] Hegarty, C., E. Powers, and B. Fonville (2004a). Accounting for timing biases between GPS, modernized GPS, and Galileo signals. *Proc. 36th Annual Precise Time and Time Interval (PTTI) Meeting*, Washington, DC, 7-9 December, pp. 307-317.

[17] Hegarty, C., E. Powers, and B. Fonville (2004b). GPS + modernized GPS + Galileo. *GPS World,* Vol. 17, No. 3, March 2004, pp. 49-54.

[18] Odijk, D., and P.J.G. Teunissen (2013). Characterization of between-receiver GPS-Galileo inter-system biases and their effect on mixed ambiguity resolution. *GPS Solutions,* Vol. 17, No. 4, pp. 521-533. DOI 10.1007/s10291-012-0298-0.

[19] Teunissen, P.J.G. (1995). The least-squares ambiguity decorrelation adjustment: a method for fast GPS integer ambiguity estimation. *Journal of Geodesy*, Vol. 70, No. 1-2, pp. 65-82. DOI 10.1007/BF00863419.

[20] Verhagen, S., and P.J.G. Teunissen (2013). The ratio test for future GNSS ambiguity resolution. *GPS Solutions,* Vol. 17, No. 4, pp. 535-548. DOI 10.1007/s10291-012-0299-z.

[21] Bona, P. (2000). Precision, cross correlation, and time correlation of GPS phase and code observations. *GPS Solutions,* Vol. 4, No. 2, pp. 3-13. DOI 10.1007/PL00012839.

[22] Euler, H.J., and C.C. Goad (1991). On optimal filtering of GPS dual-frequency observations without using orbit information. *Bull. Geod.*, Vol. 65, pp. 130-143.

[23] Verhagen, S., D. Odijk, P.J.G. Teunissen, and L. Huisman (2010). Performance improvement with low-cost multi-GNSS receivers. *Proc. 5th ESA workshop on Satellite Navigation User Equipment Technologies, NAVITEC 2010*, Noordwijk, The Netherlands, 8-10 December 2010.

[24] Teunissen, P.J.G. (1997). A canonical theory for short GPS baselines. Part I: The baseline precision. *Journal of Geodesy*, Vol. 71, No. 6, pp. 320-336. DOI 10.1007/s001900050100.

**Table 1:** Galileo vs. GPS observables: frequencies and wavelengths

| | Galileo frequencies | | | | GPS frequencies | | |
|---|---|---|---|---|---|---|---|
| | E1 | E5a | E5b | E5 | L1 | L2 | L5 |
| carrier frequency [MHz] | 1575.42 | 1176.45 | 1207.14 | 1191.795 | 1575.42 | 1227.60 | 1176.45 |
| carrier wavelength [cm] | 19.03 | 25.48 | 24.83 | 25.15 | 19.03 | 24.42 | 25.48 |

**Table 2:** Information on date, timespan, selection of Galileo and GPS satellites, cut-off elevation and sampling interval as used for datasets I and II.

| | Dataset I | Dataset II |
|---|---|---|
| Date and time | 20 March 2013 (04:05:30-06:00:00 GPST)<br>30 March 2013 (03:24:00-05:18:30 GPST) | 8 April 2013 (17:54:00-19:13:00 GPST) |
| Galileo satellites | E11-E12-E19-E20 | E19-E20 |
| GPS satellites | G5-G25-G29-G31 | G5-G7-G8-G9-G10-G26-G28 |
| Elevation cut-off | 10 deg | 45 deg |
| Sampling interval | 30 sec | 30 sec |

**Table 3:** Standard deviations (in local zenith) for the undifferenced Galileo and GPS code observables tracked by the Trimble and Septentrio receivers.

| | E1 | E5a | E5b | E5 | L1 | L2 |
|---|---|---|---|---|---|---|
| Trimble | 25 cm | 20 cm | 25 cm | 10 cm | 25 cm | 30 cm |
| Septentrio | 20 cm | 20 cm | 20 cm | 10 cm | 25 cm | 25 cm |

**Table 4:** Estimated zenith-referenced cross correlation coefficients of the Galileo code observables, based on three hours of Trimble data collected on 20 and 30 March 2013. The standard deviation of the estimated correlations is around 0.04.

| | E1/E5a | E1/E5b | E1/E5 | E5a/E5b | E5a/E5 | E5b/E5 |
|---|---|---|---|---|---|---|
| 20 March | 0.09 | 0.08 | 0.06 | 0.06 | 0.32 | 0.26 |
| 30 March | 0.11 | 0.05 | 0.10 | 0.11 | 0.28 | 0.29 |

**Table 5:** Dataset I: Position errors (mean and RMS error) for receiver CUTA, based on Galileo-only E1+E5a, GPS-only L1+L2 and Galileo&GPS E1+E5a & L1+L2, relative to a-priori known values of the position of the receiver. The position errors are computed for the case the ambiguities are float, as well as fixed (cursively printed). Time series of these position errors are depicted in Figure 6.

| | Galileo only: E1+E5a | | GPS only: L1+L2 | | Galileo&GPS: E1+E5a&L1+L2 | |
|---|---|---|---|---|---|---|
| | Ambiguity-float | *Ambiguity-fixed* | Ambiguity-float | *Ambiguity-fixed* | Ambiguity-float | *Ambiguity-fixed* |
| East | mean = -1 cm<br>RMS = 5 cm | *mean = 2 mm*<br>*RMS = 3 mm* | mean = -26 cm<br>RMS = 28 cm | *mean = 1 mm*<br>*RMS = 4 mm* | mean = -2 cm<br>RMS = 5 cm | *mean = 2 mm*<br>*RMS = 2 mm* |
| North | mean = -9 cm<br>RMS = 27 cm | *mean = -1 mm*<br>*RMS = 6 mm* | mean = -25 cm<br>RMS = 28 cm | *mean = 0 mm*<br>*RMS = 2 mm* | mean = -3 cm<br>RMS = 10 cm | *mean = 0 mm*<br>*RMS = 2 mm* |
| Up | mean = 0 cm<br>RMS = 22 cm | *mean = -7 mm*<br>*RMS = 10 mm* | mean = -29 cm<br>RMS = 38 cm | *mean = -7 mm*<br>*RMS = 10 mm* | mean = -5 cm<br>RMS = 12 cm | *mean = -6 mm*<br>*RMS = 9 mm* |

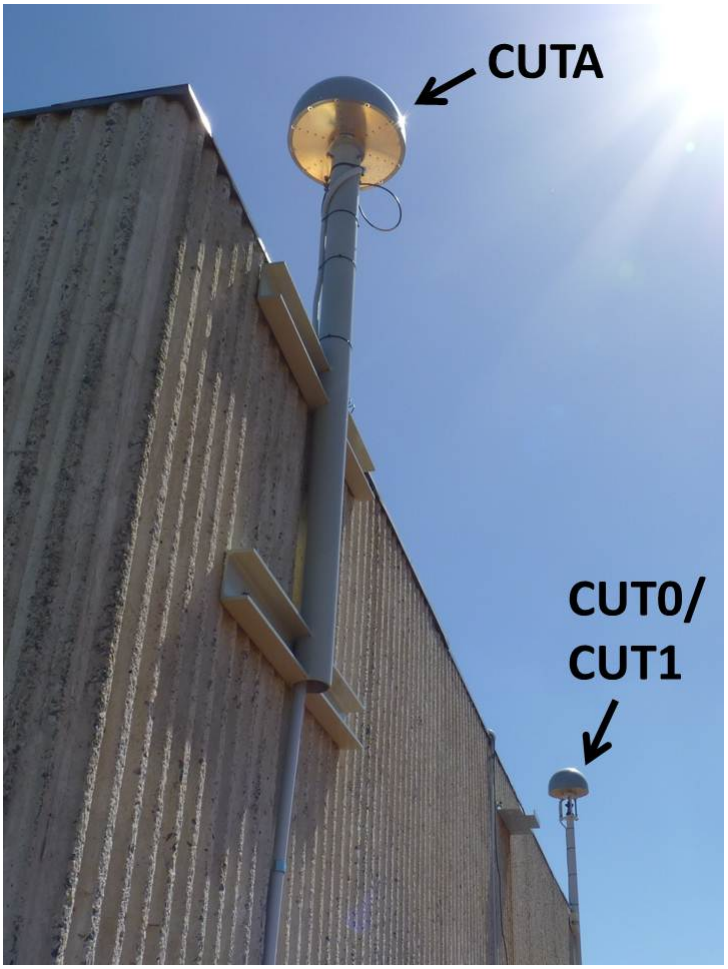


**Figure 1:** Trimble antennas on roof of Curtin University campus building 402, with inter-distance of about 8.4 m. CUTA and CUT0 are connected to Trimble NetR9 receivers, while CUT1 is connected to a Septentrio PolaRx4 receiver.

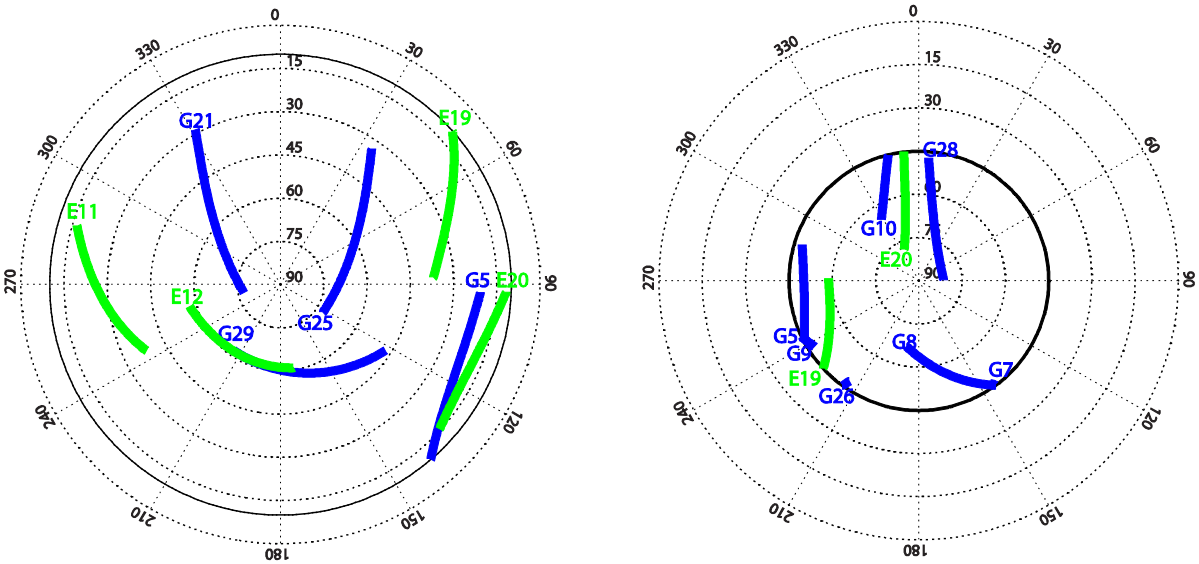


**Figure 2:** *Left (dataset I)*: Galileo-IOV&GPS sky plot, based on 4 Galileo and 4 GPS satellites, above a cut-off elevation of 10 deg, on 20/30 March 2013 at Curtin University, Perth, Australia. *Right (dataset II)*: Galileo-IOV&GPS sky plot, based on 2 Galileo and 3-4 GPS satellites (4 satellites only tracked for 53% of time), above a cut-off elevation of 45 deg, on 8 April 2013. In both plots the tracks of the Galileo satellites are coloured green and those of the GPS satellites are coloured blue. See Table 2 for the PRN numbers of the Galileo and GPS satellites appearing in the sky plots.

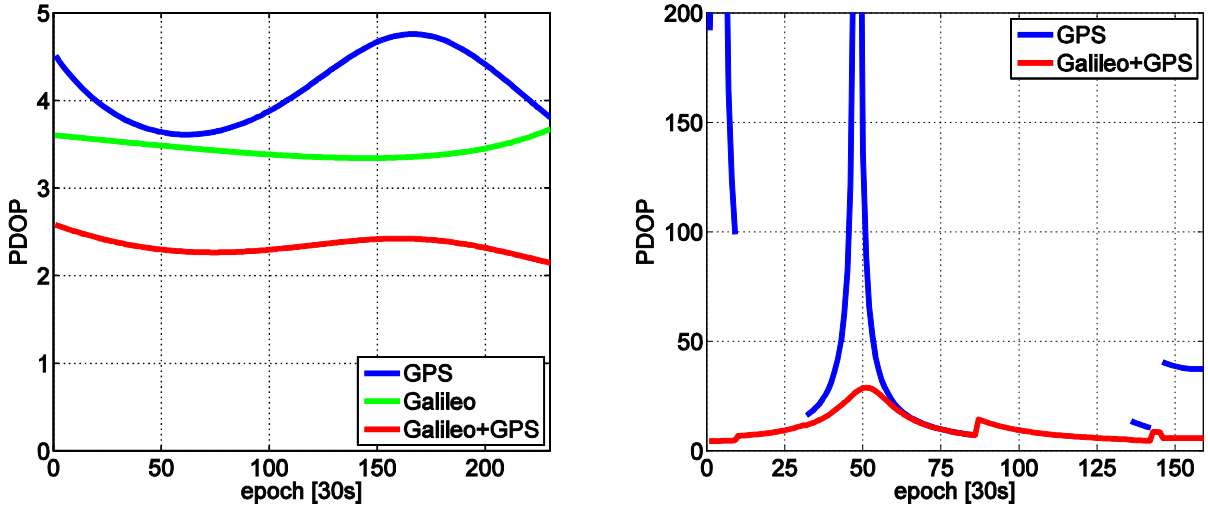


**Figure 3:** PDOPs based on GPS-only, Galileo-only and Galileo&GPS combined for dataset I (left) and for dataset II (right). For dataset I four GPS and four Galileo IOV satellites are used to compute the PDOPs, while in case of dataset II only two IOV satellites were tracked, so no PDOPs are computed for Galileo-only.

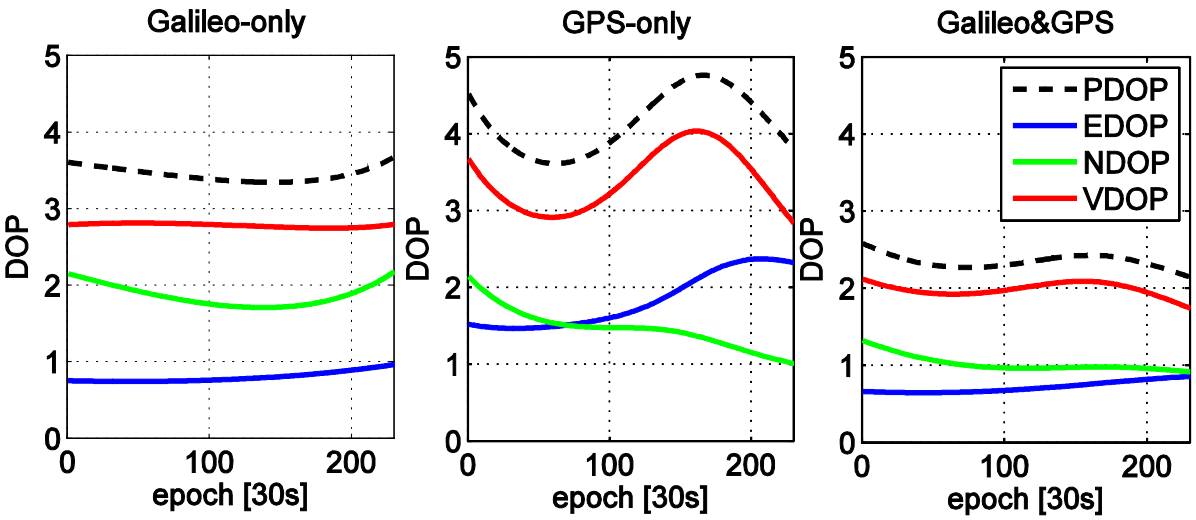


**Figure 4:** PDOPs, EDOPs, NDOPs and VDOPs for Galileo-only (left), GPS-only (middle) and Galileo&GPS (right) for dataset I, where 4 Galileo and 4 GPS satellites are used.

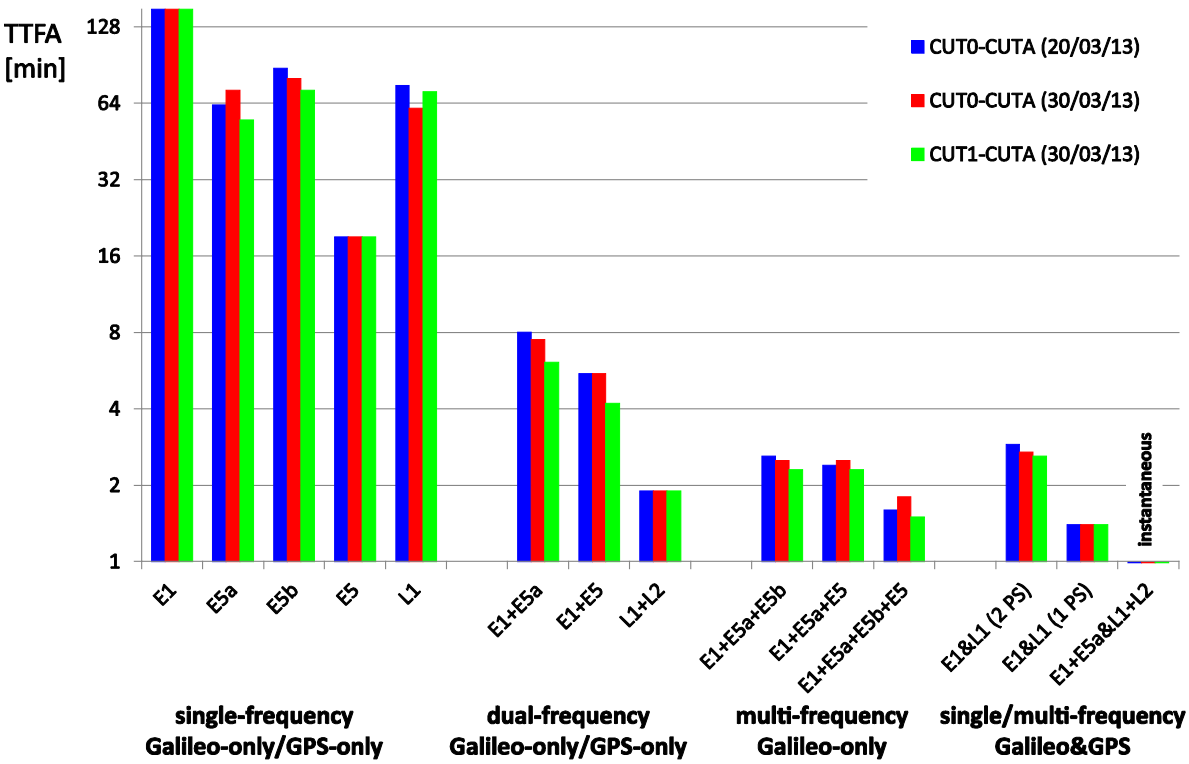


**Figure 5:** Mean times-to-fix-ambiguities (TTFA; in minutes) for the different processing strategies based on the 4-satellite Galileo IOV and 4-satellite GPS observations of dataset I, collected on baseline CUT0-CUTA on 20 March (blue bars) and 30 March (red bars) 2013, and on baseline CUT1-CUTA on 30 March 2013 (green bars). Note that the scaling of the y-axis is logarithmic. For the single/multi-frequency Galileo&GPS combined processing there are two single-frequency strategies: the first with a pivot satellite (PS) for each constellation (E1&L1; 2 PS) and the second with a common pivot satellite for both Galileo and GPS (E1&L1; 1 PS). Remark that for the single-frequency E1 and L1 cases ambiguity resolution could not be realized during the full timespan; the bars therefore take the maximum value of the y-axis. It is furthermore remarked that for the multi-frequency Galileo&GPS case the mean time-to-fix-ambiguities is just based on a single epoch (corresponds to 0.5 min) for both baselines during the two days, which explains the three small bars below the 1 minute value for E1+E5a&L1+L2.

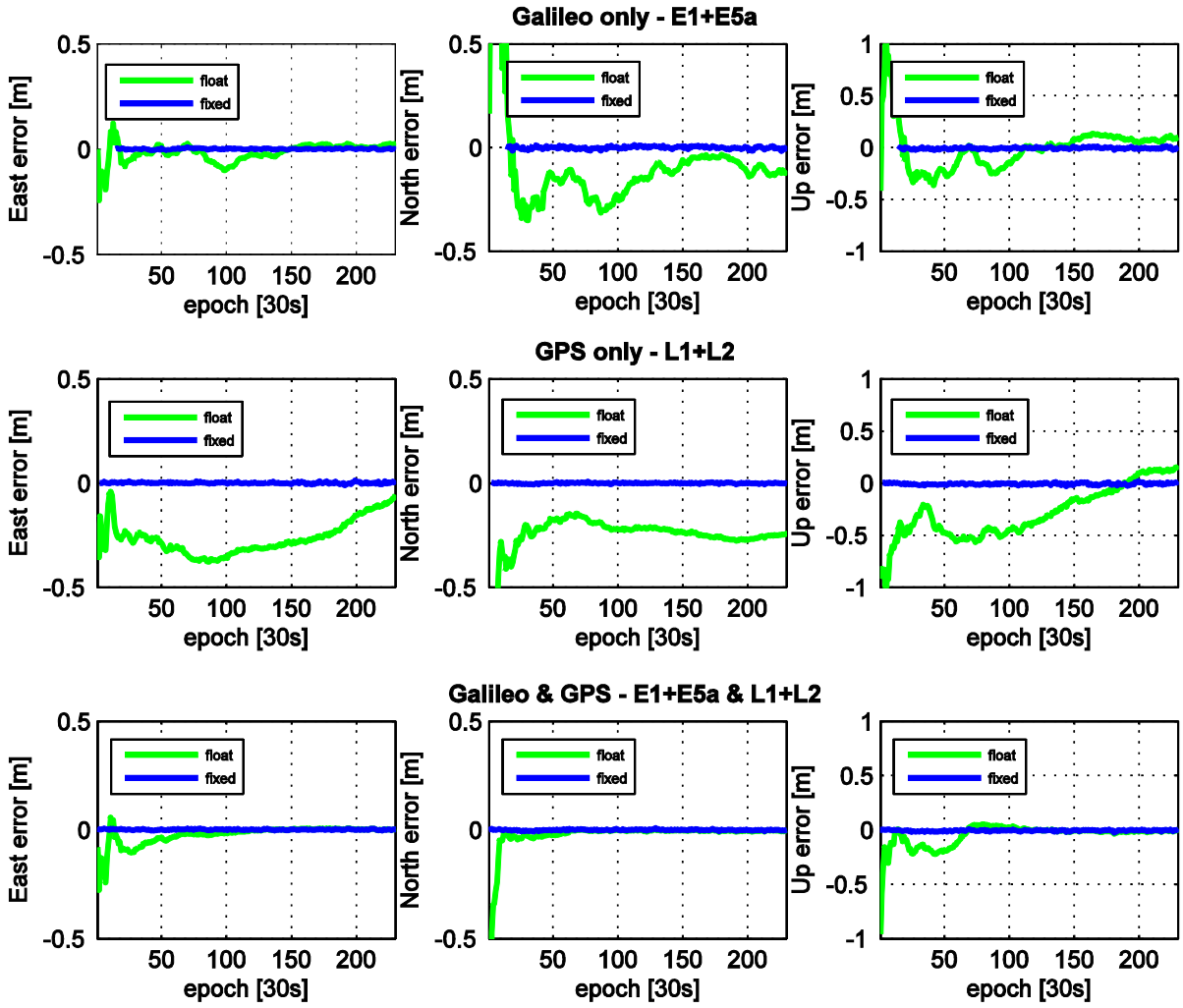


**Figure 6:** Dataset I: CUTA position (east-north-up) errors based on Galileo-only E1+E5a (top), GPS-only L1+L2 (middle) and Galileo&GPS E1+E5a & L1+L2 (bottom), estimated from the CUT1-CUTA baseline. The position errors based on float ambiguities are plotted in green; those based on fixed ambiguities are plotted in blue.

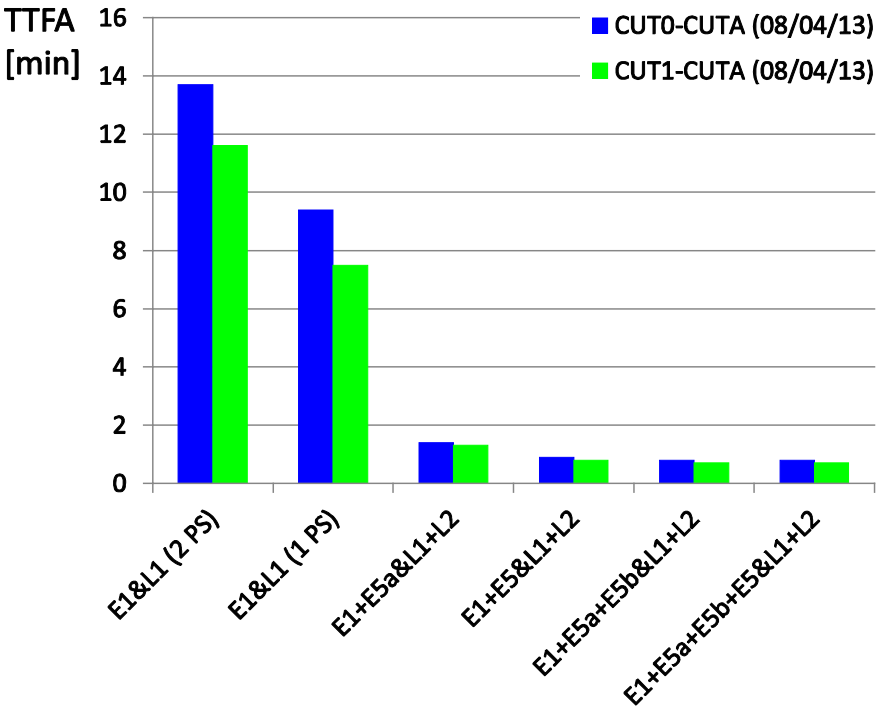


**Figure 7:** Mean times-to-fix-ambiguities (TTFA; in minutes) for the different processing strategies based on the 45-degree cut-off elevation Galileo&GPS observations of dataset II, collected on 8 April 2013 at baselines CUT0-CUTA (blue bars) and CUT1-CUTA (red bars). For the single/multi-frequency Galileo&GPS combined processing there are two single-frequency strategies: the first with a pivot satellite for each constellation (E1&L1; 2 PS) and the second with a common pivot satellite for both Galileo and GPS (E1&L1; 1 PS).

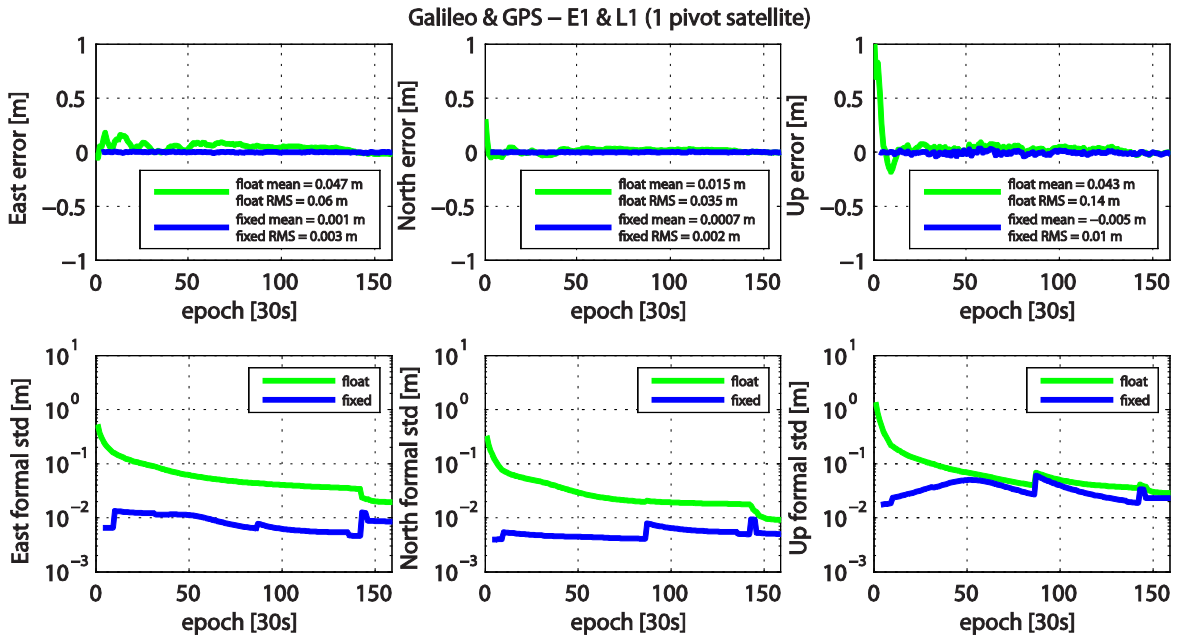


**Figure 8:** Dataset II: CUTA position (east-north-up) errors for Galileo&GPS E1&L1 with 1 pivot satellite (top) vs. formal standard deviations, for float and fixed solutions (bottom).